Strained Cyclic Disulfides Enable Cellular Uptake by Reacting with the Transferrin Receptor

Abegg, Daniel; Gasparini, Giulio; Hoch, Dominic Gregor; Shuster, Anton; Bartolami, Eline; Matile, Stefan; Adibekian, Alexander

How to cite

ABEGG, Daniel et al. Strained Cyclic Disulfides Enable Cellular Uptake by Reacting with the Transferrin Receptor. In: Journal of the American Chemical Society, 2017, vol. 139, n° 1, p. 231–238. doi: 10.1021/jacs.6b09643

This publication URL: https://archive-ouverte.unige.ch/unige:90971

Publication DOI: 10.1021/jacs.6b09643

Strained Cyclic Disulfides Enable Cellular Uptake by Reacting with the Transferrin Receptor

Daniel Abegg,[†] Giulio Gasparini,[†,‡] Dominic G. Hoch,[†] Anton Shuster,[†] Eline Bartolami,[†] Stefan Matile,[*,†] and Alexander Adibekian[*,†]

[†]School of Chemistry and Biochemistry, National Centre of Competence in Research (NCCR) Chemical Biology, University of Geneva, Geneva, Switzerland

[‡]Present address: Firmenich SA, Division of Research and Development, Geneva, Switzerland

ABSTRACT: In this study, we demonstrate that appendage of a single asparagusic acid residue (AspA tag) is sufficient to ensure efficient celullar uptake and intracellular distribution of fully unprotected peptides. We apply this new delivery method to induce apoptotic response in cancer cells using long (up to 20mer) BH_3 domain peptides. Moreover, in order to understand the molecular mechanism of the cellular uptake, we perform chemical proteomics experiments and identify the direct molecular targets of the asparagusic acid tag. Our findings document covalent bond formation between the asparagusic acid moiety and the cysteines 556 and C558 on the surface of the transferrin receptor resulting in subsequent endocytic uptake of the payload. We believe that the small size, low cellular toxicity and the efficient transferrin receptor-mediated uptake render the AspA tag highly attractive for various life science applications.

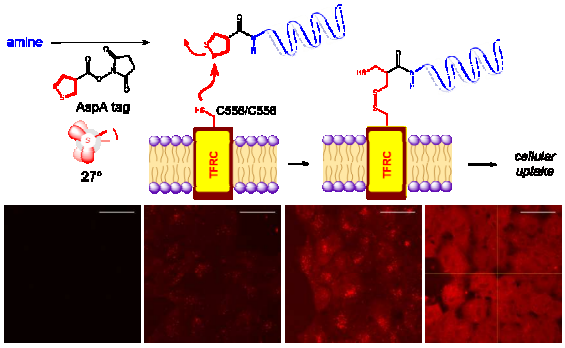

Introduction

Efficient cellular delivery remains one of the key factors to impede the development of new pharmaceuticals.[1] Large and polar molecules such as peptides, proteins, oligonucleotides and nanoparticles are usually unable to passively cross the cell membrane. Through the combined efforts of chemists, biologists, material scientists and others, various drug delivery systems have been developed to overcome this drawback. Currently, the most widely used strategies include liposomes,[2] protein cages and viral vectors,[3] PEGylation,[4] cationic polymers,[5] hydrocarbon-stapled α-helices[6] and cell-penetrating peptides (CPPs).[7] Particularly the CPPs have caused much excitement in the community since their introduction more than 20 years ago,[8] but the cell-penetrating peptides can be cytotoxic and are often trapped in the endosomal pathway thus failing to deliver the attached cargo to the desired intracellular compartment.

Thiol-mediated uptake is a conceptually novel and highly promising approach that makes use of dynamic covalent interactions with cell surface thiols to deliver hydrophilic cargos inside the cells.[9] For example, thiol-mediated uptake is believed to be largely responsible for the excellent performance of the so-called cell-penetrating poly(disulfide)s (CPDs).[9-10] Moreover, we have recently shown that even appendage of small strained cyclic disulfides suffices to transport the fluorescent dye carboxyfluorescein across the plasma membrane, and that uptake efficiency increases with disulfide ring tension, culminating with a CSSC dihedral angle of 27° in asparagusic acid.[11]

Despite the proven success of the concept of thiol-mediate uptake, the exact molecular mechanism of this intriguing process remains elusive. It is largely believed that the disulfides undergo dynamic covalent disulfide exchange with the exofacially exposed cysteine residues,[12] but the exact membrane-associated interaction partners have not been identified to date.

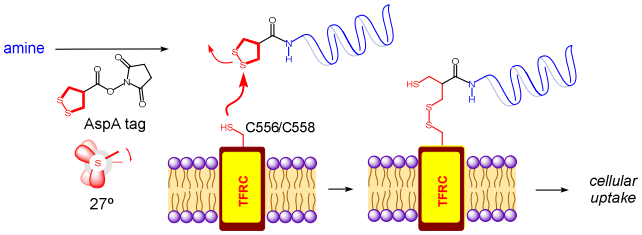

Figure 1. Schematic representation of thiol-mediated uptake of an AspA-modified peptide. Solvent-exposed cysteines on the surface of the transferrin receptor react with the strained disulfide ring (CSSC dihedral angle of 27°) of the asparagusic acid tag and the covalently bound cargo is taken up by the cell.

Herein, we demonstrate that attachment of a single asparagusic acid (AspA) residue to up to 20mer long peptides dramatically improves their transport across the cellular membrane (Figure 1). We make use of this finding to deliver proapoptotic peptides Bim BH_3 and Bak BH_3 inside multiple cancer cell lines and characterize the induced apoptotic response. Furthermore, we apply chemical proteomics strategy to identify the direct molecular targets of asparagusic acid-functionalized probes. Using complementary genetic, biochemical and cell biological techniques, we demonstrate that asparagusic acid covalently binds to transferrin receptor and is transported across the cellular membrane.

Results and Discussion

Uptake of an AspA-Tagged Heptapeptide. We began our studies with the preparation of the bifunctional model heptapeptide **1**. The *N*-terminus of the peptide was equipped with the tetramethylrhodamine (TMR) dye to enable monitoring the cellular uptake by fluorescence microscopy, whereas the ε-NH_2 group of the *C*-terminal lysine of the fully assembled and deprotected heptapeptide was reacted with asparagusic acid NHS ester. Details of the preparation and analytical data for peptide **1** and other probes mentioned below can be found in the Supporting Information. The cellular uptake was initially examined on HeLa Kyoto cells using an SDS-PAGE-based fluorescence assay (Figure 2A). Briefly, the cells were treated with H_2O, the bifunctional peptide **1** or the untagged control peptide **2** (both 1 μM) for 2 h. The cells were extensively washed, trypsinized to remove the cell membrane bound peptides and lysed. The proteomes were minimally separated by SDS-PAGE and the TMR fluorescence was detected by in-gel fluorescence scanning. Remarkably, the fluorescence was detected exclusively in the proteome originating from the cells treated with peptide **1**.

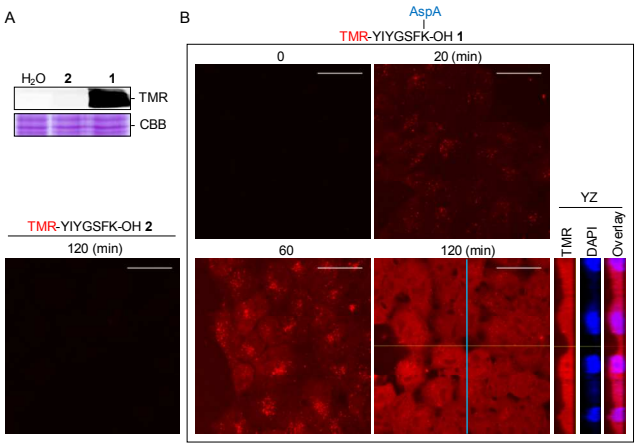

Figure 2. Cellular uptake studies with the AspA-tagged bifunctional heptapeptide **1**. (A) Fluorescent SDS-PAGE gel image showing the cellular uptake of peptides **1** and **2**. (B) Confocal images of HeLa Kyoto cells treated with the AspA-tagged heptapeptide **1** or the untagged control heptapeptide **2** for various amounts of time (n = 3; white bar indicates 30 μm). Corresponding images with DAPI-stained nuclei are shown in Figure S1. Also shown is YZ orthogonal view of z-stack images of cells treated with peptide **1** for 120 min.

To understand the uptake dynamics and the intracellular distribution of our model heptapeptide, we treated HeLa Kyoto cells with peptide **1** or **2** (both 3 μM) for various amounts of time, extensively washed and fixed the cells and investigated the uptake using confocal fluorescence microscopy (Figure 2B). Again, no uptake was detectable with control peptide **2** even after 2 h incubation time. In contrast, clear time-dependent increase in fluorescence was observed in cells treated with the AspA-tagged peptide **1**. The images taken in cells after 20 and 60 min treatment evidenced dotty, condensed localization of the peptide. Intriguingly, an entirely different pattern was observed in cells after 2 h incubation, where the fluorescence was evenly and homogeneously distributed. To ascertain that the fluorescent peptide is indeed localized inside the cells and is not, for instance, unspecifically bound to the cellular membrane, z-stacks were taken at 0.5 μm z-intervals. The z-stack images confirmed that peptide **1** was indeed uptaken and homogeneously distributed inside the HeLa Kyoto cells.

Uptake of AspA-Tagged Proapototic Peptides. Having demonstrated the uptake efficiency on the model heptapeptide, the stage was now set for much longer and bioactive peptides. The α-helical BH3 domain peptides from multidomain (such as Bax or Bak) or BH3-only (such as Bim, Bid or Bad) proapoptotic proteins are considered new and highly promising anticancer biologicals.[13] It was previously shown that Bak BH3 peptides fused with the cell-penetrating 16mer Antennapedia peptide is taken up and induces apoptosis in HeLa cells.[14] Moreover, in seminal work by Verdine and Walensky,[15] de novo designed and synthesized hydrocarbon-stapled BH3 mimetic peptides were successfully used to penetrate and kill cancer cells *in situ* and *in vivo*. Thus, we were wondering whether the same task could be accomplished by simply appending the AspA tag to the otherwise unfunctionalized and unprotected BH3 peptides. If successful, such conjugates would be clearly advantageous in terms of preparative simplicity and the small tag size (133 Da).

We synthesized the AspA-Bak BH3 conjugate **3** by simply reacting the *N*-terminus of the unprotected 16mer Bak BH3 peptide with asparagusic acid NHS ester. In addition, we prepared the control TMR-Bak BH3 peptide **4** and the bifunctional AspA- and TMR-functionalized Bak BH3 conjugate **5** for gel-based internalization experiments by adding a TMR-modified *C*-terminal lysine residue. Furthermore, we also prepared the AspA-tagged 20mer Bim BH3 conjugate **6**. We first tested the internalization of the conjugate **5** by SDS-PAGE as described above (Figure S2). While some uptake was also detectable with the TMR-Bak BH3 peptide **4**, >10 times stronger fluorescence signal was observed in lysates from cells treated with the conjugate **5** (both 1 μM). Next, we tested the cytotoxicity of conjugates **3** and **6** in four different cancer cell lines (Figures 3A, S3). As unveiled by brightfield microscopy, peptides **3** and **6** were clearly toxic in all four cell lines, whereas the cells were visibly not affected by the treatment with untagged Bak and Bim BH3 peptides. Moreover, free asparagusic acid (Figure 3A) and peptide **1** (Figure S4) also proved not toxic to cells, thus indicating that the toxicity of **3** and **6** was not caused by the AspA tag itself. However, while these experiments were performed at rather high probe concentration, it should be mentioned that both AspA-tagged BH3 peptides exhibited strong cellular toxicity at much lower concentrations in some of the cell lines. For example, we measured low micromolar EC_{50} values for AspA-Bak BH3 in invasive breast carcinoma (MCF7) and epithelial colorectal adenocarcinoma (Caco-2) cells (Figure 3B).

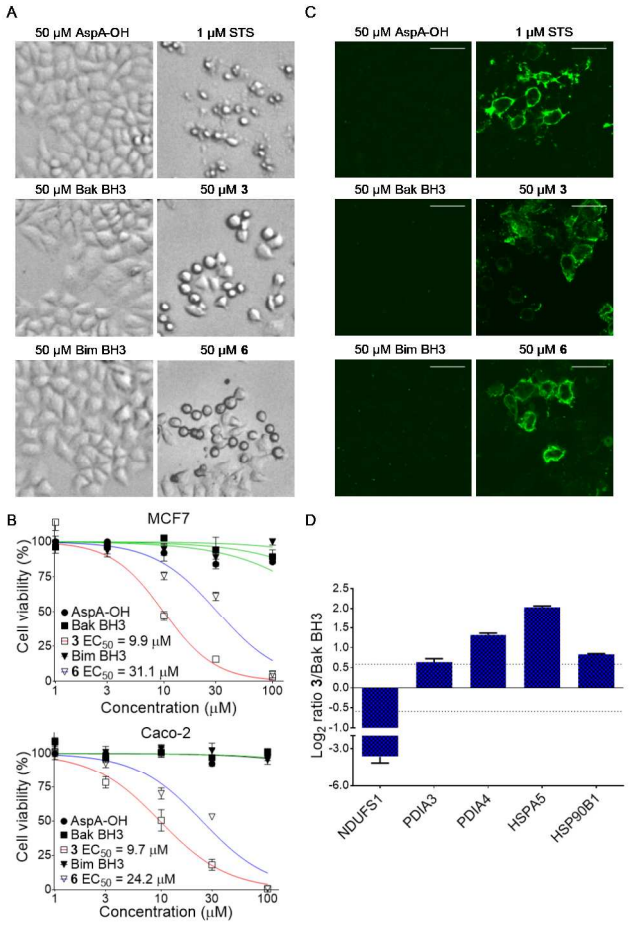

Figure 3. Treatment of cancer cell lines with proapoptotic BH3 peptides. (A) Brightfield images of HeLa Kyoto cells treated with untagged vs. AspA-tagged BH3 peptides (n = 3). Peptide **3** = AspA-GQVGRQLAIIGDDINR-OH (AspA-Bak BH3); peptide **6** = AspA-MRPEIWIAQELRRIGDEFNA-OH (AspA-Bim BH3). Asparagusic acid (AspA-OH) and staurosporine (STS) were used as controls. (B) Viability curves of MCF7 and Caco-2 cells treated with various concentrations of BH3 peptides or asparagusic acid (shown are relative values±SD; n = 3). Results from treatments of additional cell lines are presented in Figures S3, S5. (C) Detection of apoptosis in Hela Kyoto cells using annexin V staining. Confocal microscopy images are shown (n = 3; white bar indicates 30 μm). Corresponding images with DAPI-stained nuclei are presented in Figure S6. (D) Changes in cellular levels of five selected proteins following 24 h treatment of HeLa Kyoto cells with AspA-Bak BH3 **3** vs untagged Bak BH3 (shown are LFQ ratios±SD; n = 3).

Although the cell viability experiments clearly documented the cytotoxic efficacy of AspA-tagged BH3 peptides, they did not provide any prove for the anticipated proapoptotic mechanism of action. The endogenous Bak protein is known to be specifically expressed on the outer membrane of mitochondria and triggered Bak oligomerization causes mitochondrial membrane permeabilization and release of other proapoptogenic factors.[13, 16] We performed a series of additional experiments to unambiguously demonstrate that our probes indeed kill the cancer cells by causing the expected mitochondrial apoptotic response. We used annexin V staining to detect cells that have externalized phosphatidylserine on the cell surface, an event typically taking place during apoptosis.[17] As shown in Figure 3C, strong annexin V staining was observed on HeLa Kyoto cells treated with the probes **3** and **6** for 24 h, but not on cells treated with the untagged BH3 peptides or free asparagusic acid. By Western blotting, we observed increase in H2AX phosphorylation (γH2AX) in AspA-Bak BH3-treated cells, but not in cells treated with the untagged peptide or free asparagusic acid (Figure S7). γH2AX is a marker for DNA double-strand breaks, a process commonly observed during apoptosis.[18] Finally, we also performed global proteomics analysis in HeLa Kyoto cells to observe proteome-wide changes in protein levels caused by treatment with AspA-Bak BH3 **3** (Figures 3D, S8 and Table S1). In particular, we observed a drastic decrease in levels of mitochondrial NADH-ubiquinone oxidoreductase (NDUFS1), a classical sign for the mitochondrial pathway of apoptosis.[19] Moreover, several markers of the unfolded protein response (UPR) such as protein disulfide isomerases (PDIA3, PDIA4) and heat shock proteins (HSPA5, HSP90B1) were increased.[20] UPR is a cellular stress response that activates apoptosis and was previously shown to be directly modulated by endogenous Bak.[21] Collectively, these results confirm that AspA-tagged BH3 peptides act via inducing the classical mitochondrial pathway of apoptosis.

Target Identification. Having demonstrated the efficiency of the AspA tag for cellular uptake of long peptides, we sought to investigate the exact cellular mechanism responsible for the uptake of AspA-tagged peptides. Assuming that asparagusic acid must have undergone dynamic covalent disulfide exchange with solvent-exposed cysteine residues on membrane-localized proteins, we decided to try to address this question using classical chemical proteomics strategy.

For this purpose, we prepared the lysine-derived and FITC- and alkyne-tagged probe Boc-PA **7** along with its AspA-tagged derivative AA-PA **8** (Figure 4A). As expected, probe **8** was readily taken up by HeLa Kyoto cells, whereas no significant uptake was detected with the tagless derivative **7**. These results were also accurately reproducible in two additional cell lines, MCF7 and Caco-2 (Figure S9). While all live cell treatments were performed in serum-free medium, we confirmed that **8** is also efficiently, albeit more slowly, taken up by HeLa Kyoto cells in medium containing up to 10% serum (Figures S10, S11). To examine whether the probe **8** is indeed capable of forming covalent bonds with proteins, HeLa Kyoto cellular lysates were treated with 100 μM **7** or **8** for 1 h. Probe-treated proteomes were then reacted with tetramethylrhodamine (TMR) azide through CuAAC, separated by non-reducing SDS-PAGE and visualized by in-gel fluorescence scanning. The gel scan documented strong fluorescence labeling of the proteome with the AspA-tagged probe **8** but not with the control compound **7** (Figures 4B, S12). In contrast, almost no labeling was observed when reducing loading buffer for SDS-PAGE was used (Figure S13). Pretreatment with 100fold excess of the cysteine-reactive alkynyl benziodoxolone reagent JW-RF-001[22] completely abolished proteome labeling by **8**, indicating that the AspA tag indeed chemospecifically reacts with proteomic cysteines but not with other nucleophilic amino acids (Figures 4C,

S12). Finally, we confirmed that probe **8** but not probe **7** is capable of covalently engaging cysteines directly on live cells and at much lower concentration (Figures 4D, S12).

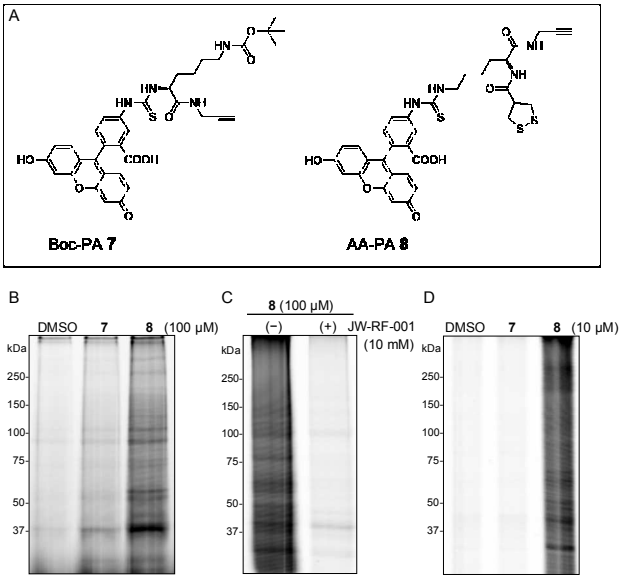

Figure 4. Gel-based profiling of proteomic targets of the AspA tag. (A) Chemical structure of lysine-derived probes Boc-PA **7** and AA-PA **8**. (B) Profiling of targets of **7** and **8** in HeLa Kyoto cell lysates. The lysates were incubated with 100 µM probe for 1 h, followed by CuAAC with TMR azide, SDS-PAGE and in-gel fluorescence scanning. (C) Competitive treatment with 100fold excess of cysteine-reactive alkynyl benziodoxolone probe JW-RF-001 to confirm that **8** modifies proteomic cysteines. (D) Treatment of live HeLa Kyoto cells with 10 µM **7** or **8**.

We next treated live cells originating from all three cell lines, HeLa Kyoto, MCF7 and Caco-2, with 10 µM **8**, but this time the probe-labeled proteomes were derivatized with biotin azide, enriched over streptavidin beads, digested and analyzed by LC-MS/MS. The identified *in situ* proteomic targets of probe **8** were filtered using three selection parameters; i) label-free quantification[23] (LFQ) intensity > 5fold than in DMSO-treated control sample, ii) GO term annotated plasma membrane localization, and iii) identified in proteomes from all three tested cell lines. This rigorous selection resulted in a short list of only five proteins with the transferrin receptor protein 1 (TFRC) as perhaps the most prominent hit (Figure 5, Table S2). TFRC is a highly abundant[24] transmembrane glycoprotein responsible for the import of transferrin-bound iron into cells by clathrin-mediated endocytosis. This highly efficient cellular uptake has extensively been exploited for drug delivery purposes.[25] Hence, we decided to investigate the AspA tag-TFRC interaction further.

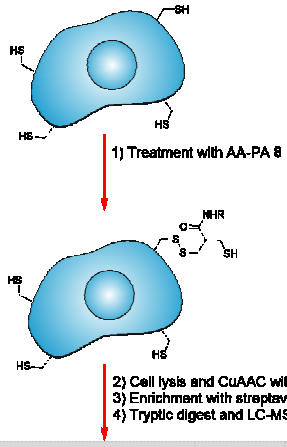

Protein name	Gene name	Average LFQ intensity		
		HeLa	MCF7	Caco-2
Transferrin receptor protein 1	TFRC	5.9E7	5.9E6	5.7E6
Cytoskeleton-associated protein 4	CKAP4	3.2E7	3.5E7	1.1E7
Scavenger receptor class B member 1	SCARB1	2.0E7	3.1E6	1.5E6
Chloride intracellular channel protein 1	CLIC1	1.6E7	1.5E7	2.3E7
Vesicle-associated membrane protein-associated protein A	VAPA	5.8E6	5.0E6	3.1E6

Figure 5. Layout and the results of the chemical enrichment experiment coupled with protein identification by LC-MS/MS. Live HeLa Kyoto, MCF7 and Caco-2 cells were treated with 10 µM **8**, lysed, derivatized by CuAAC with biotin azide, enriched over streptavidin beads, digested and analyzed by LC-MS/MS (shown are average LFQ values; $n = 4$).

Investigation of the TFRC-Mediated Uptake. Because TFRC-mediated uptake is a classic example of clathrin-mediated endocytosis, we first examined by fluorescence microscopy in HeLa Kyoto cells whether AA-PA **8** is indeed uptaken via endocytosis. Confocal images of HeLa Kyoto cells treated with **8** and Cascade Blue Dextran, an endosome-specific fluorescent probe, attributed high degree of colocalization (Figure S14). To understand the contribution of TFRC in the endocytic uptake of **8**, the transferrin receptor was knocked down using specific small interfering RNA (siRNA). Indeed, the TFRC knockdown led to a >75% diminished uptake compared to mock cells (Figure 6A). Consistently, transient overexpression of TFRC-mCherry in HeLa Kyoto cells resulted in ~45% increase in fluorescent puncta, presumably endosomes filled with **8** (Figures 6A, 6B, S15, S16). Moreover, overexpression of TFRC in HeLa Kyoto cells also led to ~30% improved cellular toxicity of AspA-Bak BH3 **3** (Figure 6C). Importantly, we confirmed by fluorescence microscopy and siRNA knockdown that the TFRC-mediated uptake of AA-PA **8** is not limited to cervical cancer HeLa Kyoto cells but also takes place in epidermoid carcinoma A431 cells, breast carcinoma MCF7 cells, colorectal adenocarcinoma Caco-2 cells, glioblastoma U-87 MG cells, and prostate adenocarcinoma PC-3 cells (Figure S17).

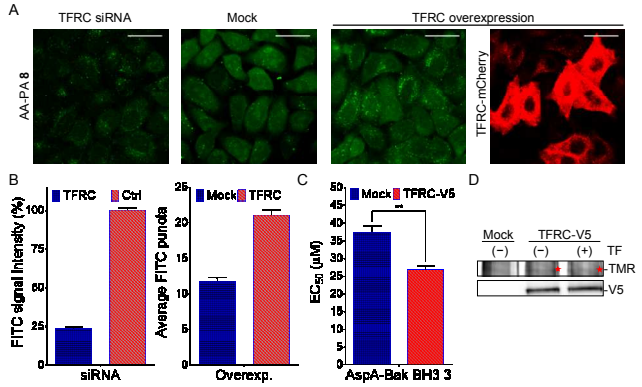

Figure 6. Investigating the role of TFRC in uptake of AspA-tagged probes. (A) Detection of the cellular uptake of AA-PA **8** upon knockdown or overexpression of TFRC. HeLa Kyoto cells were treated with 3 μM **8** for 1 h. Confocal microscopy images are shown (n = 3; white bar indicates 30 μm). (B) Quantification of AA-PA uptake upon knockdown (left) and overexpression (right) of TFRC (shown are average values±SEM, n = 3). (C) EC_{50} values measured in mock and TFRC-overexpressing cells after treatment with AspA-Bak BH3 **3** (shown are average values±SD, n = 3). **P < 0.005 by two-sided Student's t-test. (D) Gel-based detection of TFRC labeling by 100 μM AA-PA **8**. TFRC-V5 was overexpressed in Hela Kyoto cells. The labeling was performed on lysates prepared from mock or TFRC-V5 overexpressing cells and with or without pretreatment with transferrin (TF). Red asterisks mark the TFRC band.

Finally, we sought to determine the exact AspA binding site on the transferrin receptor. TFRC is a dimer held together by two disulfide bonds and each monomer can bind one iron-transferrin complex. Our proteomics results suggested direct binding of AA-PA **8** to TFRC. To confirm this finding, we overexpressed TFRC in HeLa Kyoto cells, lysed the cells and treated the lysate with **8** followed by CuAAC with TMR azide, SDS-PAGE and in-gel fluorescence scanning (Figure 6D). The gel image showed direct labeling of the overexpressed TFRC by **8**. Interestingly, pretreatment with a large excess of transferrin, the natural TFRC ligand, didn't compete the labeling of the receptor, suggesting that AA-PA binds to a cysteine residue presumably localized outside of the transferrin-binding site of the receptor. Each TFRC monomer contains four solvent exposed cysteine residues: C89, C98, C556 and C558. C89 and C98 are engaged in the intermolecular disulfide bridges between both monomers and are therefore essential for the functionality of the dimeric receptor.[26] C556 and C558 are located within a β-sheet region and form disulfide in the dimeric, transferrin-bound TFRC[27] but appear to be present as free thiols in the monomeric form of the receptor (Figures 7A and S18).[28] This can be explained by the fact that binding of iron-transferrin complex to TFRC is known to induce global conformational changes in its extracellular domain.[27] Thus, C556 and C558 could potentially serve as reaction partners for asparagusic acid. Unfortunately, expressed single mutants C556S and C558S were still able to bind AA-PA **8** by gel and also the uptake of **8** in cells expressing the single mutants was not significantly reduced compared to the overexpressed WT TFRC (Figures 7B, 7C and S19). Therefore, we also created and overexpressed the TFRC double mutant C556S/C558S. We first confirmed that the C556S/C558S mutant is still a fully functional TFRC receptor through inspection of the intracellular localization and also by using a fluorescent transferrin uptake assay (Figure S20). At this time, however, AA-PA failed to bind to the expressed mutant TFRC in our gel-based experiment (Figure 7D). Hence, also the cells expressing the double mutant showed greatly diminished uptake compared to cells with overexpressed WT TFRC and the level of uptake was similar to the mock cells (Figures 7B, 7C, S21).

In summary, our results demonstrate that the AspA-tagged probes are taken up by cells mainly via the transferrin receptor-mediated endocytosis and that C556 and C558 on the surface of TFRC likely serve as binding sites for the AspA tag.

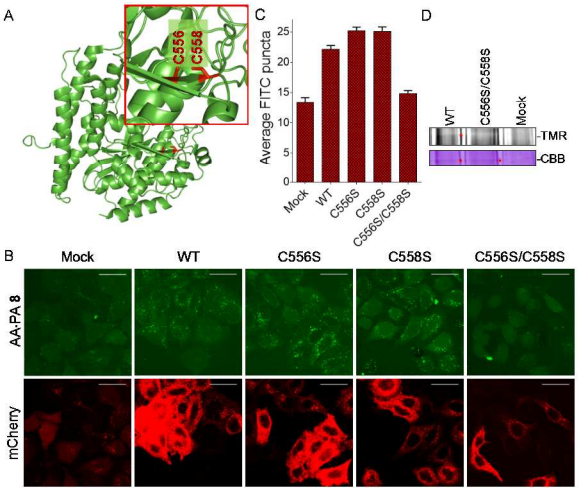

Figure 7. Determination of the exact site of binding of AA-PA **8** on TFRC. (A) Protein structure of *H. sapiens* TFRC (PDB: 3KAS) with C556 and C558 displayed in red. The image was created using PyMOL (V1.7.2.1). (B) Detection of the cellular uptake of AA-PA **8** upon overexpression of WT, single (C556S, C558S) or double (C556S/C558S) mutant TFRC. HeLa Kyoto cells were treated with 3 μM **8** for 1 h. Confocal microscopy images are shown (n = 3; white bar indicates 30 μm). (C) Quantification of AA-PA uptake upon overexpression of WT and mutant TFRC variants (shown are average values±SEM, n = 3). (D) Gel-based detection of labeling of WT and double mutant (C556S/C558S) TFRC by 100 μM AA-PA **8.** Red asterisks mark the TFRC band.

Conclusions

We have herein demonstrated that appendage of a single asparagusic acid residue is sufficient to ensure efficient cellular uptake and intracellular distribution of fully unprotected peptides. We utilized this new delivery method to induce apoptotic response in cancer cells using long (up to 20mer) BH3 domain peptides. Furthermore, we conducted chemical enrichment experiments combined with mass spectrometry detection to identify the direct molecular targets of the asparagusic acid tag. Finally, we performed a series of biological experiments that revealed direct covalent bond formation between the AspA tag and cysteines 556 and C558 on the surface of the transferrin receptor resulting in efficient

cellular uptake of the AspA-modified probes in six different cell lines.

Several general attributes render the AspA tag attractive for various life science applications. Firstly, asparagusic acid is not toxic to cells even at higher concentrations. Secondly, the AspA tag is small and is thus less likely to alter the biological properties of the modified peptides. Preparation of AspA-tagged peptides is very simple and does not require advanced synthetic organic skills. Finally, the AspA tag is orthogonal to and thus can be combined with other popular peptide modifications such as CPPs and hydrocarbon staples to achieve even more efficient cellular uptake.

Classical transferrin receptor-mediated drug delivery requires payload conjugation to transferrin to form a large macromolecular complex that is then being bound and internalized by the receptor. The AspA tag renders the preparation of cargo-transferrin conjugates unnecessary by directly binding to the transferrin receptor *in situ*. Once the plasma membrane is passed, the payload is conveniently detached from the receptor through reduction of the disulfide bridge presumably by the lysosomal thiol reductase. AspA-tagged peptides are able to reach different intracellular compartments, although the exact mechanism of the endosomal escape remains to be clarified. Given the ubiquitous expression of the transferrin receptor in all mammalian tissues, including the blood-brain barrier, it is also tempting to speculate about the effectivity of using AspA conjugates directly *in vivo*. Because the transferrin receptor is known to be highly overexpressed in multiple cancer forms[29] (Figure S22), AspA conjugates may find clinical application as anticancer therapeutics. This scenario is currently being investigated in our laboratories.

Another important question that needs clarification is whether the TFRC-mediated uptake mechanism is also utilized by the so-called cell-penetrating poly(disulfide)s (CPDs). Preliminary results indicate mixed uptake mechanism presumably combining thiol-mediated uptake with CPP-like direct translocation, either across the plasma membrane or for endosomal escape. These results will be reported in due course.

ASSOCIATED CONTENT

Experimental details. This material is available free of charge via the Internet at http://pubs.acs.org.

AUTHOR INFORMATION

Corresponding Authors

alexander.adibekian@unige.ch, stefan.matile@unige.ch

Notes

The authors declare no competing financial interests.

ACKNOWLEDGMENT

We thank the Bioimaging Platform for confocal microscopy measurements, the NMR platform for services, and the University of Geneva, the National Centre of Competence in Research (NCCR) Chemical Biology and the Swiss NSF for financial support.

REFERENCES

1. (a) Langer, R., Drug delivery and targeting. *Nature* **1998,** *392* (6679), 5-10; (b) Yoo, J. W.; Irvine, D. J.; Discher, D. E.; Mitragotri, S., Bio-inspired, bioengineered and biomimetic drug delivery carriers. *Nat Rev Drug Discov* **2011,** *10* (7), 521-535; (c) Malakoutikhah, M.; Teixido, M.; Giralt, E., Shuttle-Mediated Drug Delivery to the Brain. *Angew Chem Int Edit* **2011,** *50* (35), 7998-8014.

2. Allen, T. M.; Cullis, P. R., Liposomal drug delivery systems: From concept to clinical applications. *Adv Drug Deliver Rev* **2013,** *65* (1), 36-48.

3. (a) Ma, Y. J.; Nolte, R. J. M.; Cornelissen, J. J. L. M., Virus-based nanocarriers for drug delivery. *Adv Drug Deliver Rev* **2012,** *64* (9), 811-825; (b) Schoonen, L.; van Hest, J. C. M., Functionalization of protein-based nanocages for drug delivery applications. *Nanoscale* **2014,** *6* (13), 7124-7141.

4. Haag, R.; Kratz, F., Polymer therapeutics: Concepts and applications. *Angew Chem Int Edit* **2006,** *45* (8), 1198-1215.

5. (a) Liechty, W. B.; Kryscio, D. R.; Slaughter, B. V.; Peppas, N. A., Polymers for Drug Delivery Systems. *Annu Rev Chem Biomol* **2010,** *1*, 149-173; (b) Priegue, J. M.; Crisan, D. N.; Martinez-Costas, J.; Granja, J. R.; Fernandez-Trillo, F.; Montenegro, J., In Situ Functionalized Polymers for siRNA Delivery. *Angewandte Chemie* **2016,** 55 (26), 7492-5; (c) Li, M.; Ehlers, M.; Schlesiger, S.; Zellermann, E.; Knauer, S. K.; Schmuck, C., Incorporation of a Non-Natural Arginine Analogue into a Cyclic Peptide Leads to Formation of Positively Charged Nanofibers Capable of Gene Transfection. *Angew Chem Int Edit* **2016,** 55 (2), 598-601; (d) Wexselblatt, E.; Esko, J. D.; Tor, Y., On Guanidinium and Cellular Uptake. *J Org Chem* **2014,** *79* (15), 6766-6774.

6. (a) Walensky, L. D.; Bird, G. H., Hydrocarbon-Stapled Peptides: Principles, Practice, and Progress. *J Med Chem* **2014,** *57* (15), 6275-6288; (b) Cromm, P. M.; Spiegel, J.; Grossmann, T. N., Hydrocarbon Stapled Peptides as Modulators of Biological Function. *Acs Chem Biol* **2015,** *10* (6), 1362-1375.

7. (a) Bechara, C.; Sagan, S., Cell-penetrating peptides: 20 years later, where do we stand? *Febs Lett* **2013,** *587* (12), 1693-1702; (b) Cascales, L.; Henriques, S. T.; Kerr, M. C.; Huang, Y. H.; Sweet, M. J.; Daly, N. L.; Craik, D. J., Identification and Characterization of a New Family of Cell-penetrating Peptides. *J Biol Chem* **2011,** *286* (42), 36932-36943.

8. (a) deRonde, B. M.; Birke, A.; Tew, G. N., Design of Aromatic-Containing Cell-Penetrating Peptide Mimics with Structurally Modified pi Electronics. *Chem-Eur J* **2015,** *21* (7), 3013-3019; (b) Herce, H. D.; Garcia, A. E.; Cardoso, M. C., Fundamental Molecular Mechanism for the Cellular Uptake of Guanidinium-Rich Molecules. *J Am Chem Soc* **2014,** *136* (50), 17459-17467; (c) Stanzl, E. G.; Trantow, B. M.; Vargas, J. R.; Wender, P. A., Fifteen Years of Cell-Penetrating Guanidinium-Rich Molecular Transporters: Basic Science, Research Tools, and Clinical Applications. *Accounts Chem Res* **2013,** *46* (12), 2944-2954; (d) Brock, R., The Uptake of Arginine-Rich Cell-Penetrating Peptides: Putting the Puzzle Together. *Bioconjugate Chem* **2014,** *25* (5), 863-868; (e) Eggimann, G. A.; Blattes, E.; Buschor, S.; Biswas, R.; Kammer, S. M.; Darbre, T.; Reymond, J. L., Designed cell penetrating peptide dendrimers efficiently internalize cargo into cells. *Chem Commun* **2014,** *50* (55), 7254-7257.

9. Gasparini, G.; Bang, E. K.; Molinard, G.; Tulumello, D. V.; Ward, S.; Kelley, S. O.; Roux, A.; Sakai, N.; Matile, S., Cellular Uptake of Substrate-Initiated Cell-Penetrating Poly(disulfide)s. *J Am Chem Soc* **2014,** *136* (16), 6069-6074.

10. (a) Torres, A. G.; Gait, M. J., Exploiting cell surface thiols to enhance cellular uptake. *Trends Biotechnol* **2012,** *30* (4), 185-190; (b) Oupicky, D.; Li, J., Bioreducible Polycations in Nucleic Acid Delivery: Past, Present, and Future Trends. *Macromol Biosci* **2014,** *14* (7), 908-922; (c) Lin, C.; Engbersen, J. F. J., The role of the disulfide group in disulfide-based polymeric gene carriers. *Expert Opin Drug Del* **2009,** *6* (4), 421-439; (d) Bang, E. K.; Lista, M.; Sforazzini, G.; Sakai, N.; Matile, S., Poly(disulfide)s. *Chem Sci* **2012,** *3* (6), 1752-1763; (e) Kim, T. I.; Kim, S. W., Bioreducible polymers for gene delivery. *React Funct Polym* **2011,** *71* (3), 344-349; (f) Zeng, H. X.; Little, H. C.; Tiambeng, T. N.; Williams, G. A.; Guan, Z. B., Multifunctional Dendronized Peptide Polymer Platform for Safe and Effective siRNA Delivery. *J Am Chem Soc* **2013,** *135* (13), 4962-4965; (g) Drake, C. R.; Aissaoui, A.; Argyros, O.; Thanou, M.; Steinke, J. H. G.; Miller, A. D., Examination of the effect of increasing the number of intra-disulfide amino functional groups on the performance of small molecule cyclic polyamine disulfide vectors. *J Control Release* **2013,** *171* (1), 81-90; (h) Brulisauer, L.; Kathriner, N.; Prenrecaj, M.; Gauthier, M. A.; Leroux, J. C., Tracking the Bioreduction of Disulfide-Containing Cationic Dendrimers. *Angew Chem Int Edit* **2012,** *51* (50), 12454-12458; (i) Bang, E. K.; Gasparini, G.; Molinard, G.; Roux, A.; Sakai, N.; Matile, S., Substrate-Initiated Synthesis of Cell-Penetrating Poly(disulfide)s. *J Am Chem Soc* **2013,** *135* (6), 2088-2091; (j) Son, S.; Namgung, R.; Kim, J.; Singha, K.; Kim, W. J., Bioreducible Polymers for Gene Silencing and Delivery. *Accounts Chem Res* **2012,** *45* (7), 1100-1112; (k) Balakirev, M.; Schoehn, G.; Chroboczek, J., Lipoic acid-derived amphiphiles for redox-controlled DNA delivery. *Chem Biol* **2000,** *7* (10), 813-819; (l) Yu, C.; Qian, L.; Ge, J.; Fu, J.; Yuan, P.; Yao, S. C.; Yao, S. Q., Cell-Penetrating Poly(disulfide) Assisted Intracellular Delivery of Mesoporous Silica Nanoparticles for Inhibition of miR-21 Function and Detection of Subsequent Therapeutic Effects. *Angewandte Chemie* **2016,** *55* (32), 9272-6; (m) Hashim, P. K.; Okuro, K.; Sasaki, S.; Hoashi, Y.; Aida, T., Reductively Cleavable Nanocaplets for siRNA Delivery by Template-Assisted Oxidative Polymerization. *J Am Chem Soc* **2015,** *137* (50), 15608-15611.

11. Gasparini, G.; Sargsyan, G.; Bang, E. K.; Sakai, N.; Matile, S., Ring Tension Applied to Thiol-Mediated Cellular Uptake. *Angew Chem Int Edit* **2015,** *54* (25), 7328-7331.

12. Gasparini, G.; Bang, E. K.; Montenegro, J.; Matile, S., Cellular uptake: lessons from supramolecular organic chemistry. *Chem Commun* **2015,** *51* (52), 10389-10402.

13. Willis, S. N.; Adams, J. M., Life in the balance: how BH3-only proteins induce apoptosis. *Curr Opin Cell Biol* **2005,** *17* (6), 617-625.

14. Holinger, E. P.; Chittenden, T.; Lutz, R. J., Bak BH3 peptides antagonize Bcl-x(L) function and induce apoptosis through cytochrome c-independent activation of caspases. *J Biol Chem* **1999,** *274* (19), 13298-13304.

15. (a) Walensky, L. D.; Kung, A. L.; Escher, I.; Malia, T. J.; Barbuto, S.; Wright, R. D.; Wagner, G.; Verdine, G. L.; Korsmeyer, S. J., Activation of apoptosis in vivo by a hydrocarbon-stapled BH3 helix. *Science* **2004,** *305* (5689), 1466-1470; (b) Edwards, A. L.; Wachter, F.; Lammert, M.; Huhn, A. J.; Luccarelli, J.; Bird, G. H.; Walensky, L. D., Cellular Uptake and Ultrastructural Localization Underlie the Proapoptotic Activity of a Hydrocarbon-stapled BIM BH3 Peptide. *Acs Chem Biol* **2015,** *10* (9), 2149-2157.

16. Willis, S. N.; Chen, L.; Dewson, G.; Wei, A.; Naik, E.; Fletcher, J. I.; Adams, J. M.; Huang, D. C. S., Proapoptotic Bak is sequestered by Mcl-1 and Bcl-x(L), but not Bcl-2, until displaced by BH3-only proteins. *Gene Dev* **2005,** *19* (11), 1294-1305.

17. Koopman, G.; Reutelingsperger, C. P. M.; Kuijten, G. A. M.; Keehnen, R. M. J.; Pals, S. T.; Vanoers, M. H. J., Annexin-V for Flow Cytometric Detection of Phosphatidylserine Expression on B-Cells Undergoing Apoptosis. *Blood* **1994,** *84* (5), 1415-1420.

18. Rogakou, E. P.; Nieves-Neira, W.; Boon, C.; Pommier, Y.; Bonner, W. M., Initiation of DNA fragmentation during apoptosis induces phosphorylation of H2AX histone at serine 139. *J Biol Chem* **2000,** *275* (13), 9390-9395.

19. Ricci, J. E.; Munoz-Pinedo, C.; Fitzgerald, P.; Bailly-Maitre, B.; Perkins, G. A.; Yadava, N.; Scheffler, I. E.; Ellisman, M. H.; Green, D. R., Disruption of mitochondrial function during apoptosis is mediated by caspase cleavage of the p75 subunit of complex I of the electron transport chain. *Cell* **2004,** *117* (6), 773-786.

20. Schroder, M.; Kaufman, R. J., The mammalian unfolded protein response. *Annu Rev Biochem* **2005,** *74*, 739-789.

21. Hetz, C.; Bernasconi, P.; Fisher, J.; Lee, A. H.; Bassik, M. C.; Antonsson, B.; Brandt, G. S.; Iwakoshi, N. N.; Schinzel, A.; Glimcher, L. H.; Korsmeyer, S. J., Proapoptotic BAX and BAK modulate the unfolded protein response by a direct interaction with IRE1 alpha. *Science* **2006,** *312* (5773), 572-576.

22. Abegg, D.; Frei, R.; Cerato, L.; Hari, D. P.; Wang, C.; Waser, J.; Adibekian, A., Proteome-Wide Profiling of Targets of Cysteine reactive Small Molecules by Using Ethynyl Benziodoxolone Reagents. *Angew Chem Int Edit* **2015,** *54* (37), 10852-10857.

23. Cox, J.; Hein, M. Y.; Luber, C. A.; Paron, I.; Nagaraj, N.; Mann, M., Accurate Proteome-wide Label-free Quantification by Delayed Normalization and Maximal Peptide Ratio Extraction, Termed MaxLFQ. *Mol Cell Proteomics* **2014,** *13* (9), 2513-2526.

24. Wisniewski, J. R.; Ostasiewicz, P.; Dus, K.; Zielinska, D. F.; Gnad, F.; Mann, M., Extensive quantitative remodeling of the proteome between normal colon tissue and adenocarcinoma. *Mol Syst Biol* **2012,** *8*.

25. (a) Daniels, T. R.; Delgado, T.; Helguera, G.; Penichet, M. L., The transferrin receptor part II: Targeted delivery of therapeutic agents into cancer cells. *Clin Immunol* **2006,** *121* (2), 159-176; (b) Rosen, C. B.; Kodal, A. L. B.; Nielsen, J. S.; Schaffert, D. H.; Scavenius, C.; Okholm, A. H.; Voigt, N. V.; Enghild, J. J.; Kjems, J.; Torring, T.; Gothelf, K. V., Template-directed covalent conjugation of DNA to native antibodies, transferrin and other metal-binding proteins. *Nat Chem* **2014,** *6* (9), 804-809.

26. Cheng, Y.; Zak, O.; Alsen, P.; Harrison, S. C.; Walz, T., Structure of the human transferrin receptor-transferrin complex. *Cell* **2004,** *116* (4), 565-576.

27. Eckenroth, B. E.; Steere, A. N.; Chasteen, N. D.; Everse, S. J.; Mason, A. B., How the binding of human transferrin primes the transferrin receptor potentiating iron release at endosomal pH. *P Natl Acad Sci USA* **2011,** *108* (32), 13089-13094.

28. Abraham, J.; Corbett, K. D.; Farzan, M.; Choe, H.; Harrison, S. C., Structural basis for receptor recognition by New World hemorrhagic fever arenaviruses. *Nat Struct Mol Biol* **2010,** *17* (4), 438-U76.

29. Uhlen, M.; Fagerberg, L.; Hallstrom, B. M.; Lindskog, C.; Oksvold, P.; Mardinoglu, A.; Sivertsson, A.; Kampf, C.; Sjostedt, E.; Asplund, A.; Olsson, I.; Edlund, K.; Lundberg, E.; Navani, S.; Szigyarto, C. A.; Odeberg, J.; Djureinovic, D.; Takanen, J. O.; Hober, S.; Alm, T.; Edqvist, P. H.; Berling, H.; Tegel, H.; Mulder, J.; Rockberg, J.; Nilsson, P.; Schwenk, J. M.; Hamsten, M.; von Feilitzen, K.; Forsberg, M.; Persson, L.; Johansson, F.; Zwahlen, M.; von Heijne, G.; Nielsen, J.; Ponten, F., Tissue-based map of the human proteome. *Science* **2015,** *347* (6220).